ACS APPLIED MATERIALS & INTERFACES

RESEARCH ARTICLE

www.acsami.org

Novel Thieno-[3,4-b]-Pyrazines Cored Dendrimers with Carbazole Dendrons: Design, Synthesis, and Application in Solution-Processed Red Organic Light-Emitting Diodes

Jiuyan Li,*,† Qing Li,‡ and Di Liu‡

†State Key Laboratary of Fine Chemicals, School of Chemical Engineering, ‡School of Chemistry, Dalian University of Technology, 2 Linggong Road, Dalian 116024, China

Supporting Information

ABSTRACT: A series of novel red-emitting thieno-[3,4-*b*]-pyrazine-cored molecules containing oligo-carbazole dendrons (called **C1-TP**, **C2-TP**) are synthesized. Their photophysical, electrochemical, and electroluminescent properties are investigated. The peripheral carbazolyl units facilitate the hole transporting ability and inhibit the intermolecular interactions, but quench the fluorescence of the thieno-[3,4-*b*]-pyrazine core through Intramolecular Charge Transfer (ICT). Introduction of a polyphenyl spacer between the core and the first generation carbazole dendrons, i.e., **C-DTP**, decreases the ICT efficiency. In addition to providing the site-isolation effect on the planar emissive core, these bulky dendrons enable these molecules to be solution processable. As a result, efficient OLEDs with saturated red emission are fabricated by spin coating technique using these dendritic materials as nondoped emitting layer. **C-DTP** exhibits much better device performance than **C1-TP** and **C2-TP**, while the small molecular reference compound containing neither the spacer nor the carbazole dendrons (**TP**) fails to transmit pure red emission under identical conditions. A brightness of 925 cd m^{-2} and a luminous efficiency of 0.53 cd A^{-1} are obtained for **C-DTP**, which are comparable with OLEDs fabricated from thieno-[3,4-*b*]-pyrazine-based counterparts by the vacuum deposition method or those assembled with other red fluorescent dendrimers via the solution processing method.

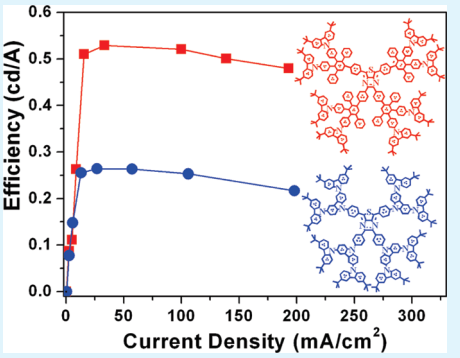

KEYWORDS: organic light-emitting diodes, solution processable, thieno-[3, 4-*b*]-pyrazine, dendrimer, carbazole dendron, red

INTRODUCTION

Organic light-emitting devices (OLEDs) have been drawing broad attentions due to their practical applications in both large-area flat-panel displays and solid-state lighting. For light-emitting materials used in OLEDs, a large Stokes shift and a high luminescent quantum yield are required if an efficient light output from the device is desired. Otherwise the severe self-absorption caused by spectral overlap between the absorption and emission will adversly affect light output.[1] Among the three primary color light-emitting materials and devices, the red one still lag behind in terms of luminescent efficiency and lifetime.[2−4] It is, thus, strongly desired to develop highly efficient red emitters with good merits such as a large Stokes shift for the application in OLEDs. The thieno-[3,4-*b*]-pyrazine based molecules were proved to be red fluorophores with large Stokes shifts of over 100 nm. There are two major absorption bands for this family of molecules. One is narrow but strong band centered at 320 nm and another is broad but weak absorption ranging from 450 to 530 nm. The weak absorption at longer wavelength range has a tiny overlap with the fluorescence, consequently resulting in a large Stokes shift. In 2002, Tao and co-workers reported a group of thieno[3,4-b]pyrazine-containing molecules and fabricated non-doped red OLEDs by vacuum evaporation technique.[4] However, there has been no record of using thieno-[3,4-*b*]-pyrazine derivatives to fabricate OLEDs via the solution processing technique.

It is well-established that the solution processing is the most favorable fabrication technique of OLEDs for low cost and large-area displays and lighting.[5,6] In addition to light-emitting polymers, the dendritic molecules have ascended to be another type of optoelectronic material for solution processable OLEDs because of the inherent topological features. The emissive core of dendritic molecules is surrounded by branched dendrons, which prevents self-aggregation and concentration-quenching in the solid state.[7−9] To act as nondoped emitters, the dendrons are usually charge transporting groups. Carbazole is one widely used hole transporting group because of its low ionization potential and thus strong electron donating nature.[10] Carbazole-containing molecules usually exhibit relatively intense luminescence, high chemical and morphological stabilities,[11,12] and can undergo reversible oxidation processes which makes them suitable as hole carriers.[13] So far, a lot of carbazole-based materials have been developed for application in electroluminescence devices.[8,14−19]

Received: March 14, 2011
Accepted: May 17, 2011
Published: May 17, 2011

Scheme 1. Chemical Structures of the Compounds in Present Study

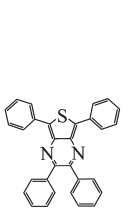

TP

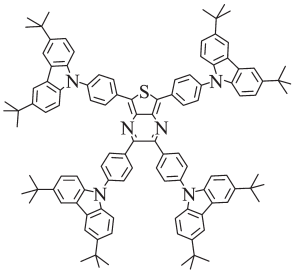

C1-TP

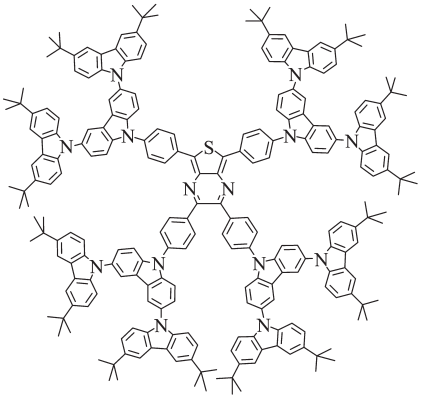

C2-TP

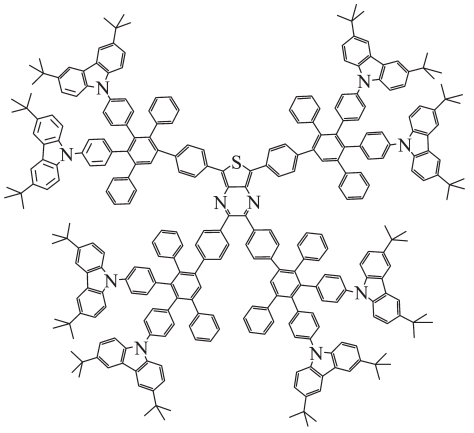

C-DTP

Our aim is to develop solution-processable thieno-[3,4-*b*]-pyrazine-cored dendrimers which are capable of acting as nondoped emitters to achieve efficient saturated red emission in OLEDs. In this paper, we report the design, synthesis and light-emitting properties of a group of novel thieno-[3,4-*b*]-pyrazine-based molecules, **TP**, **C1-TP**, **C2-TP** and **C-DTP** (Scheme 1). Thieno-[3,4-*b*]-pyrazine was selected as the emissive core considering its large Stokes shift and the intrinsic saturated red fluorescence. Oligo-carbazoles were used as functional dendrons for the following purposes: (1) to generate proper charge transporting ability[20−25] so as to make the target molecules suitable as nondoped emitters, (2) to form nonplanar molecules for good solubility and preventing intermolecular interaction, and (3) to provide sufficient molecular weight and viscosity to make the products suitable for solution process. However, the n-type nature of thieno-[3,4-*b*]-pyrazine and the p-type feature of carbazole make the intramolecular charge transfer (ICT) unavoidable, which consequently quenches the core emission.[26,27] Accordingly, higher-generation carbazole dendrons and even a polyphenyl spacer were utilized (in **C2-TP** and **C-DTP**) in this study to control the ICT extent. The results revealed that the ICT effect and the favorable contributions are so well balanced in **C-DTP** molecule that it produced the best light-emission performance in OLEDs among all these analogues.

EXPERIMENTAL SECTION

General Information. All the chemicals for the synthesis are analytical grade and used as received without further purification. ^{1}H NMR spectra were recorded on a Bruker AvanceII (400 MHz) and Varian INOVA spectrometer (400 MHz). ^{13}C NMR spectra were recorded on a Varian INOVA spectrometer (100 MHz). Mass spectra were recorded on a GC-Tof MS (Micromass, UK) mass spectrometer for TOF-MS-EI, on a MALDI micro MX (Waters, USA) for MALDI-TOF-MS and on a HP 1100 LC-MSD (USA) mass spectrometer for API-ES-MS. The fluorescence and UV−vis absorption spectra measurements were performed on a Perkin-Elmer LS55 fluorescence spectrometer and a Perkin-Elmer Lambda 35 UV−visible spectraphotometer, respectively. The phosphorescence quantum yields were determined against rhodamine B as the standard (Φ_F = 0.97 in ethanol). Melting point were recorded on a WRS-1B number melting point instrument (Shanghai precision and scientific instrument CO.)

OLED Fabrication and Measurements. The precleaned ITO glass substrates were treated by UV-ozone for 20 min. A 40 nm thick PEDOT: PSS film was first deposited on the ITO glass substrates, and baked at 120 °C for 40 min in air. The emitting layer were spin-coated from the solution of **C2-TP** or **C-DTP** in chlorobenzene on top of PEDOT:PSS film. The **TP** or **C1-TP** film and other organic layers were deposited by vacuum evaporation in a vacuum chamber with a base pressure of less than 10^{-6} Torr. Finally a thin layer of LiF (1 nm) and 100 nm of Al were vacuum deposited on top of organic layers as cathode. The EL spectra, CIE coordinates, and current−voltage-luminance characteristics were measured with computer-controlled Spectrascan PR 705 photometer and a Keithley 236 source-measure-unit. All the measurements were carried out at room temperature under ambient conditions.

Cyclic Voltammetry Measurements. Electrochemical measurements were made by using a conventional three-electrode configuration and an electrochemical workstation (BAS100B, USA) at a scan rate of 50 mV s^{-1}. A glass carbon working electrode, a Pt-wire counter electrode, and a Saturated Calomel Electrode (SCE) as reference

electrode were used. All measurements were made at room temperature on samples dissolved in dichloromethane, with 0.1 M tetra-n-ethylammonium tetrafluoroborate as the electrolyte. The solutions were deoxygenated with argon. The highest occupied molecular orbital (HOMO), the lowest unoccupied molecular orbital (LUMO) and the band gap (E_g) of the compounds were calculated using the equations listed below.

$$\text{HOMO} = -e(E_{ox}^{onset} + 4.4)\ [\text{eV}]$$

$$\text{LUMO} = E_g + \text{HOMO}\ [\text{eV}]$$

Synthesis of Compounds. *2,5-Dibromo-3,4-dinitrothiophene (**1**).* Concentrated sulfuric acid (100 mL) and fuming sulfuric acid (30% SO_3, 100 mL) were combined in a flask equipped with a mechanical stirrer and cooled with an ice bath. 2,5-Dibromothiophene (53.8 g, 0.222 mol) was then added at a temperature below 20 °C. Concentrated nitric acid (35 mL) was then carefully added to keep the temperature under 30 °C. Once the addition was completed, the mixture was allowed to react for an additional 3 h and then poured over 800 g of ice. Upon the melting of the ice, the solid residue was recovered by vacuum filtration and washed well with water to produce a light yellow powder. Recrystallization with methanol gave 69.3 g (94%) of analytically pure material; Mp 135.8−136.7 °C.

*2,5-Bis-phenyl-3,4-dinitro-thiophene (**2a**) and 2,5-Bis-(4-bromophenyl)-3,4-dinitro-thiophene (**2b**).* To a solution of compound **1** (5 g, 15 mmol), phenylboronic acid or 4-bromophenylboronic acid (33 mmol) and [$Pd(PPh_3)_4$] (450 mg, 375 mmol) in toluene (250 mL), a mixture of methanol (50 mL) and 2 M K_2CO_3 aqueous solution (65 mL) was added. The reaction mixture was refluxed for 8 h under nitrogen and then diluted with water. The organic layer was separated, and the aqueous layer was extracted with CH_2Cl_2 (3 × 50 mL). After the CH_2Cl_2 extraction was washed with brine (1 × 50 mL) and dried over $MgSO_4$, it was combined with the original organic reaction solution. The resulted organic solution was evaporated under reduced pressure and the residue was purified by column chromatography on silica gel (CH_2Cl_2/petroleum ether) to yield bright yellow solids.

2a: yield 37%, used directly for synthesis of **3a**.

2b: yield 41.2%. ^{1}H NMR (400 MHz, $CDCl_3$): δ = 7.65 (d, J = 8 Hz, 4 H; Ar−H), 7.39 (d, J = 8 Hz, 4 H; Ar−H); MS (TOF-MS-EI, m/z): Calcd. for $C_{16}H_8Br_2N_2O_4S$: 481.86; found 481.86.

*2,5-Bis-phenyl-3,4-thiophene-3,4-diamine (**3a**) and 2,5-Bis-(4-bromo-phenyl)-3,4-thiophene-3,4-diamine (**3b**).* To a suspension of **2a** or **2b** (10 mmol) and tin powder (9.4 g, 800 mmol) in ethanol (150 mL), concentrated HCl acid was added and the mixture was subsequently stirred under nitrogen at 50 °C for 6 h. The homogeneous solution was poured into ice water and made alkaline with aqueous NaOH. The organic layer was separated, the aqueous layer was extracted with CH_2Cl_2 (3 × 50 mL), and the dried extraction was combined with the original organic solution. The organic mixture was evaporated under reduced pressure. The white solid was recrystallized from CH_2Cl_2/petroleum ether to yield the analytically pure sample.

3a: yield 80.2%, not characterized.

3b: yield 85.2%. MS (TOF-MS-EI, m/z): calcd for $C_{16}H_{12}Br_2N_2S$, 421.91; found, 421.91.

*2,3-Bis-phenyl-5,7-bis-phenyl-thieno[3,4-b]pyrazine (**TP**) and 2,3-Bis-(4-bromo-phenyl)-5,7-bis(4-bromo-phenyl)-thieno[3,4-b]pyrazine (**4**).* Compound **3** (1 mmol) and 1, 2-bis-phenyl-ethane-1,2-dione or 1,2-bis-(4-bromo-phenyl)-ethane-1,2-dione (1 mmol) were dissolved in dry $CHCl_3$ (60 mL) and a catalytic amount of *p*-toluenesulfonic acid was added. The mixture was stirred at room temperature overnight. The red solid were collected by filtration and dried under a vacuum. Recrystallization with $CHCl_3$/petroleum ether gave analytically pure material.

TP: yield 65.1%. ^{1}H NMR (400 MHz, $CDCl_3$): δ = 8.3 (d, 4 H, J = 8 Hz; Ar−H), 7.56 (d, 4 H, J = 8 Hz; Ar−H), 7.51 (t, 4 H; Ar−H), 7.37−7.33 (m, 8 H, Ar−H); MS (TOF-MS-EI, m/z): calcd for $C_{30}H_{20}N_2S$, 440.13; found, 440.13.

4: yield 84.3%. ^{1}H NMR (400 MHz, $CDCl_3$): δ = 8.13 (d, 4 H, J = 7.6 Hz; Ar−H), 7.63 (d, 4 H, J = 8 Hz; Ar−H), 7.53 (d, 4 H, J = 8 Hz; Ar−H), 7.40 (d, 4 H, J = 7.6 Hz; Ar−H); MS (TOF-MS-EI, m/z): calcd for $C_{30}H_{16}Br_4N_2S$, 751.78; found, 751.78.

*2,3-Bis-(4-(trimethylsilylethynyl)phenyl)-5,7-bis(4-(trimethylsilyl)-ethynylphenyl)-thieno[3,4-b]pyrazine (**5**).* Compound **4** (500 mg, 0.67 mmol) was dissolved in a degassed mixture of triethylamine (20 mL) and absolute THF (10 mL) under nitrogen. [$PdCl_2(PPh_3)_2$] (93 mg, 5 mol %), CuI (63 mg, 0.33 mmol), and PPh_3 (86 mg, 0.33 mmol) were then added under a flow of nitrogen. After the flask was sealed with a septum, trimethylsilylethyne (0.45 mL) was injected. The reaction mixture was stirred at 45 °C for 48 h, and then poured into an equal volume of CH_2Cl_2 and filtered. The solvent was removed and the crude product was purified by column chromatography on silica gel (CH_2Cl_2/petroleum ether) to afford red solid (400 mg, 73.4%). ^{1}H NMR (400 MHz, $CDCl_3$): δ = 8.23 (d, 4 H, J = 8.4 Hz; Ar−H), 7.56 (d, 4 H, J = 8.4 Hz; Ar−H), 7.46−7.41 (q, 8 H; Ar−H), 0.278 (s, 18 H; CH_3), 0.271 (s, 18 H; CH_3); MS (MALDI-TOF, m/z): calcd for $C_{50}H_{52}N_2SSi_4$, 824.29; found 824.18.

*2,3-Bis-(4-ethynyl-phenyl)-5,7-bis(4-ethynyl-phenyl)-thieno[3,4-b]-pyrazine (**6**).* Compound **5** (400 mg, 0.48 mmol) and NH_4F (143 mg, 3.9 mmol) were dissolved in THF (10 mL) under nitrogen. A solution of *n*-Bu_4NF (19 mg, 0.07 mmol) in THF (5 mL) was added by injection. The mixture was stirred at room temperature for 2 h. Then the solvents were removed under vacuum, and the crude product was purified by column chromatography on silica gel (CH_2Cl_2/petroleum ether) to give a red solid **6** (255 mg, 98%). ^{1}H NMR (400 MHz, $CDCl_3$): δ = 8.27 (d, 4 H, J = 8.4 Hz; Ar−H), 7.61 (d, 4 H, J = 8.4 Hz; Ar−H), 7.48 (s, 8 H; Ar−H), 3.19 (s, 2 H; C≡CH), 3.17(s, 2 H; C≡CH); MS (TOF-MS-EI, m/z): calcd for $C_{38}H_{20}N_2S$, 536.13; found, 536.13.

*3,6-Di(tert-butyl)carbazole (**7**).* **7** was prepared according to the literature procedures.[17,28]

*3,6-Di(tert-butylcarbazolyl)carbazole (**8**).* A mixture of **7** (6.1 g, 22 mmol), 3,6-diiodo-9-(toluene-4- sulfonyl)carbazole (5.7 g, 10 mmol), CuI (0.4 g), and K_2CO_3 (4.1 g) in nitrobenzene (15 mL) was heated to 170 °C and stirred for 24 h under nitrogen. After cooling to room temperature, CH_2Cl_2 was added and the mixture was filtered. Solvent was removed under reduced pressure, and the residue together with an excess of KOH (8 g) was dissolved in a mixture of dioxane (40 mL) and water (10 mL), and refluxed overnight. After extraction with CH_2Cl_2, the organic layer was washed with dilute hydrochloric acid and water, dried over Na_2SO_4, and then filtered. After the solvent was removed, the residue was purified by column chromatography on silica gel (petroleum ether/ethyl acetate) to give **8** with a yield of 56% (4.0 g). MS (MSD, m/z): calcd for $C_{52}H_{55}N_3$, 721.44; found, 721.44.

*1,2-Bis[4-(tert-butylcarbazolyl)phenyl]ethane-1,2-dione (**9**).* A mixture of 4,4′-Dibromobenzil (500 mg, 1.36 mmol), tert-butylcarbazole (835 mg, 3 mmol), CuI (52 mg), K_2CO_3 (650 mg), 18-crown-6 (90 mg), and 1,2-dichlorobenzene (10 mL) was refluxed under nitrogen for 5 h. After cooling, the solvents were removed under reduced pressure, and the crude product was purified by column chromatography on silica gel (CH_2Cl_2/petroleum ether) to give a bright yellow solid **9** (270 mg, 26%). ^{1}H NMR (400 MHz, $CDCl_3$): δ = 8.29 (d, 4 H, J = 8.4 Hz; Ar−H), 8.13 (s, 4 H; Ar−H), 7.82 (d, 4 H, J = 8.4 Hz; Ar−H), 7.49 (s, 8 H; Ar−H), 1.47 (s, 36 H; CH_3); MS (API-ES, m/z): calcd for $C_{54}H_{56}N_2O_2$, 764.4; found, 764.5.

*3,4-Bis[4-(tert-butylcarbazolyl)phenyl]-2,5-diphenylcyclopenta-2,4-dienone (**10**).* Compound **9** (765 mg, 1 mmol) and diphenyl acetone (210 mg, 1 mmol) were dissolved in ethanol (20 mL) and were heated to reflux. KOH (62 mg, 1.1 mmol) in 3 mL ethanol was added, and the reaction mixture was refluxed for 2 h. The reaction mixture was then cooled to 4 °C, and the precipitate was removed via suction filtration and

Scheme 2. Synthetic Routes for TP, C1-TP, C2-TP and C-DTP[a]

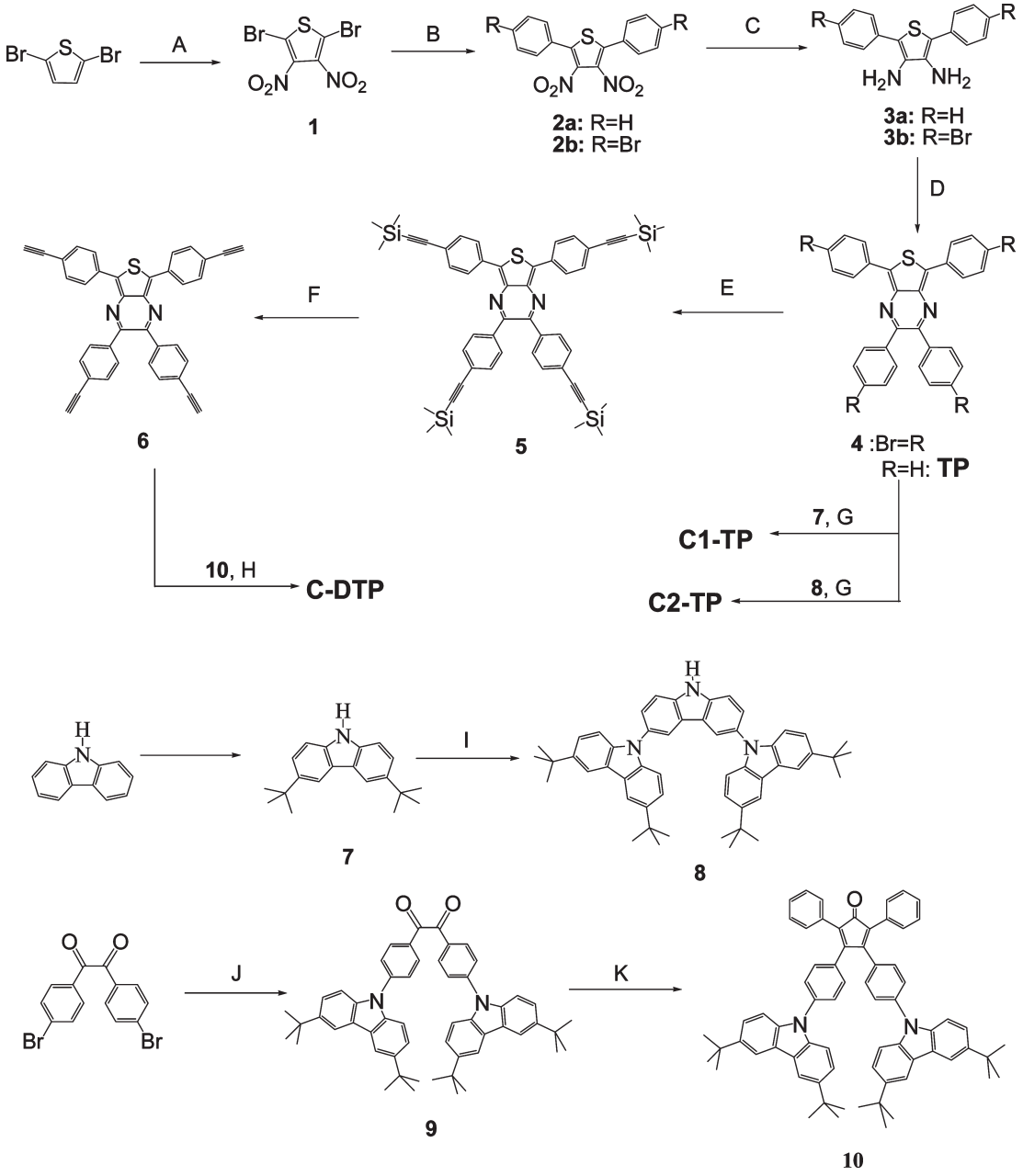

[a] Conditions and reagents: (A) fuming H_2SO_4, conc. HNO_3, rt; (B) phenylboronic acid or 4-bromophenylboronic acid, $Pd(PPh_3)_4$, K_2CO_3, toluene-MeOH, reflux, N_2; (C) Sn, HCl, EtOH, 50°C,N_2; (D) *p*-toluenesulfonic acid, dry $CHCl_3$, 1,2-bis-phenyl-ethane-1,2-dione or 1,2-bis-(4-bromophenyl)-ethane-1,2-dione, rt; (E) NEt_3, $PdCl_2(PPh_3)_2$, PPh_3, CuI, THF, trimethylsilylethyne, 45°C,N_2; (F) NH_4F, *n*-Bu_4NF, THF, rt, N_2; (G) compd (7 or 8), CuI, K_2CO_3, 18-crown-6, 1,2-dichlorobenzene, reflux, N_2; (H) *o*-xylene, Cp (**10**), reflux, N_2; (I) 3,6-diiodo-9-(toluene-4- sulfonyl)carbazole, CuI, K_2CO_3, nitrobenzene, reflux, N_2; then KOH, dioxane, rt; (J) *t*-butylcarbazole, CuI, K_2CO_3, 18-Crown-6, 1,2-dichlorobenzene, reflux, N_2; (K) diphenylacetone, KOH, EtOH, reflux.

collected as the crude product. The brown solid was recrystallized from $CHCl_3$/ethanol to yield an analytically pure product (522 mg, 55.7%). ^{1}H NMR (400 MHz, $CDCl_3$): δ = 8.12 (s, 4 H; Ar−H), 7.51 (d, 4 H, J = 8 Hz; Ar−H), 7.44 (d, 4 H, J = 8.8 Hz; Ar−H), 7.39−7.31 (m, 14 H; Ar−H), 7.25 (d, 4 H, J = 8.8 Hz; Ar−H), 1.44 (s, 36 H; CH_3); MS ((MALDI-TOF, m/z): calcd for $C_{69}H_{66}N_2O$, 938.52; found, 938.39.

C1-TP. A mixture of **4** (500 mg, 0.66 mmol), **7** (967 mg, 3.46 mmol), CuI (52 mg), K_2CO_3 (1.29 mg), 18-crown-6 (90 mg), and 1,2-dichlorobenzene (20 mL) was refluxed under nitrogen for 48 h. After cooling, the solvents were removed in vacuum, and the crude product was purified by column chromatography on silica gel (CH_2Cl_2/petroleum ether) and then recrystallization to give a red solid **C1-TP** (370 mg, 36%). ^{1}H NMR (400 MHz, $CDCl_3$): δ = 8.62 (d, 4 H, J = 8 Hz; Ar−H), 8.18 (d, 8 H, J = 12 Hz; Ar−H), 7.96 (d, 4 H, J = 8 Hz; Ar−H), 7.80 (d, 4 H, J = 8 Hz; Ar−H), 7.70 (d, 4 H, J = 8 Hz; Ar−H), 7.53 −7.46 (m, 16 H; Ar−H), 1.49 (s, 36 H; CH_3), 1.46 (s, 36 H; CH_3). MS (MALDI-TOF, m/z): calcd for $C_{110}H_{112}N_6S$, 1548.87; found, 1548.88. Elemental anal. Calcd for $C_{110}H_{112}N_6S$: C, 85.23; H, 7.28; N, 5.42. Found: C, 84.87; H, 7.02; N, 5.17.

Table 1. Photophysical and Electrochemical Data of the Red Dyes

compd	λ_{abs} (nm) toluene	λ_{abs} (nm) CH_2Cl_2	λ_{em} (nm) toluene/CH_2Cl_2	Stokes Shift (nm) toluene/CH_2Cl_2	Φ (%) [a] toluene/CH_2Cl_2	HOMO/LUMO (eV)[b]	E_g (eV) [c]
TP	323, 489	320, 483	597/605	108/122	60.5/28.4	−5.40/−3.18	2.22
C1-TP	298, 336, 346, 452, 542	297, 334, 346, 433, 521	639/646	97/125	17.3/6.8	−5.28/−3.28	2.00
C2-TP	299, 335, 347, 516	298, 336, 348, 511	630/636	114/125	26.7/7.6	−5.32−-3.29	2.03
C-DTP	298, 335, 348, 519	298, 336, 348, 516	613/623	94/107	42.5/24	−5.30/−3.26	2.04

[a] Related to rhodamine B as the standard (Φ=0.97 in ethanol). [b] HOMO energy were calculated with reference to saturated calomel electrode (SCE). [c] Energy band gap, determined from solid films by absorption edge technique.

C2-TP. **C2-TP** was synthesized with a similar method to that of **C1-TP**. A mixture of **4** (500 mg, 0.66 mmol), **8** (2.27 mg, 3.15 mmol), CuI (52 mg), K_2CO_3 (1.29 mg), 18-crown-6 (90 mg) and 1,2-dichlorobenzene (20 mL) was refluxed under nitrogen for 6 days. After cooling, the solvents were removed under vacuum, and the crude product was purified by column chromatography on silica gel (CH_2Cl_2/petroleum ether) to give a red solid **C2-TP** (661 mg, 30%). ^{1}H NMR (400 MHz, $CDCl_3$): δ = 8.81 (d, 2 H, J = 8 Hz; Ar−H), 8.76 (d, 1 H, J = 8 Hz; Ar−H), 8.73 (d, 1 H, J = 8 Hz; Ar−H), 8.28−8.26 (m, 4 H; Ar−H), 8.24−8.21 (m, 4 H; Ar−H), 8.19−8.12 (m, 18 H; Ar−H), 8.01 (d, 4 H, J = 8 Hz; Ar−H), 7.95 (d, 4 H, J = 8 Hz; Ar−H), 7.83−7.76 (m, 8 H; Ar−H), 7.67−7.6 (m, 8 H; Ar−H), 7.49−7.44 (m, 12 H; Ar−H), 7.41−7.38 (m, 6 H; Ar−H), 7.36−7.3 (m, 10 H; Ar−H), 7.27 (d, 6 H, J = 8 Hz; Ar−H), 1.45 (s, 72 H; CH_3), 1.43 (s, 72 H; CH_3). ^{13}C NMR (100 MHz, $CDCl_3$): δ = 142.8, 140.3, 140.2, 140.1, 139.9, 131.5, 131.3, 129.8, 126.9, 126.5, 124.5, 124.4, 123.8, 123.3, 119.6, 116.4, 111.4, 109.2, 34.9 (Ar−C), 32.2 (CH_3); MS (MALDI-TOF, m/z): Calcd for $C_{238}H_{232}N_{14}S$, 3317.83; found, 3317.8054. Elemental anal. Calcd for $C_{238}H_{232}N_{14}S$: C, 86.09; H, 7.04; N, 5.91. Found: C, 85.72; H, 6.89; N, 5.59.

C-DTP. A solution of **6** (200 mg, 0.37 mmol) and **10** (1.79 mmol) in *o*-xylene (10 mL) was stirred and refluxed for 48 h under nitrogen. After cooling to room temperature, the solvent was evaporated under reduced pressure. The crude product was purified by column chromatography on silica gel (CH_2Cl_2/petroleum ether) to give pure product as red powder (1.35 g, 87.5%). ^{1}H NMR (400 MHz, $CDCl_3$): δ = 8.17 (d, 4 H, J = 12 Hz; Ar H), 8.09−8.05 (m, 16 H; Ar−H), 7.79 (d, 4 H, J = 12 Hz; Ar−H), 7.42 (d, 4 H, J = 8 Hz; Ar−H), 7.39 (d, 4 H, J = 8 Hz; Ar−H), 7.34−7.27 (m, 24 H; Ar−H), 7.25−7.0 (q, 12 H; Ar−H), 7.18−7.16 (m, 32 H; Ar−H), 7.10−7.05 (m, 30 H; Ar−H), 7.02 (d, 6 H, J = 8 Hz; Ar−H), 6.98 (d, 4 H, J = 8 Hz; Ar−H), 1.42 (s, 72 H; CH_3), 1.40 (s, 72 H; CH_3). ^{13}C NMR (100 MHz, $CDCl_3$): δ = 152.3, 142.9, 141.7, 142.8, 141.7, 141.6, 141.5, 141.3, 141.2, 140.8, 139.9, 139.8, 139.6, 139.5, 139.4, 139.3, 139.2, 139.1, 137.4, 136.1, 136, 135.7, 233.1, 131.9, 131.8, 131.3, 130.8, 130.3, 130.1, 129.9, 129.8, 129.1, 128.1, 127.7, 127.6, 127.4, 126.9, 126.4, 126.9, 126.4, 126.2, 125.9, 125.8, 123.7, 123.4, 116.3, 109.2, 34.9 (Ar−C), 32.2 (CH_3); MS (MALDI-TOF, m/z): calcd for $C_{310}H_{284}N_2S$, 4178.23; found, 4180.6172. Elemental anal. Calcd for $C_{310}H_{284}N_2S$: C, 89.04; H, 6.85; N, 3.35. Found: C, 88.61; H, 6.48; N, 3.16.

RESULTS AND DISCUSSION

Design and Synthesis. The synthetic procedures for the parent compound **TP** and the dendritic compounds **C1-TP, C2-TP** and **C-DTP** were shown in Scheme 2. The thieno-[3,4-b]-pyrazine emissive core was easily formed by cyclo-condensation of 2,5-bisaryl-3,4-bisamino-thiophene and 1,2-bisaryl-ethane-1,2-dione in the presence of 4-methylbenzenesulfonic acid. The first and second generation dendrimers **C1-TP** and **C2-TP** were synthesized by a convergent method. The oligocarbazoles **7** and **8** were prepared according to the literature methods.[17,28] These dendritic oligocarbazoles were then coupled with **4** by Ullmann reactions to give the corresponding dendritic compounds **C1-TP** and **C2-TP**. In order to enlarge the dendron dimension, the polyphenylene groups were introduced as spacers between the thieno-[3,4-*b*]-pyrazine core and the carbazole periphery, to form the target molecule **C-DTP**.[26] The polyphenylene spacer was formed through Diels−Alder cycloaddition of the functional tetraphenylcyclopentadienone (Cp) **10** to the terminal ethynyl groups in intermediate **6**.[29,30] Cp **10** was synthesized by condensing diphenylacetone with the intermediate **9**, which was prepared by coupling the corresponding carbozole groups with 4,4′-dibromobenzil.[31] Then, **C-DTP** are formed by Diels−Alder reaction of core molecule **6** with Cp **10** in *o*-xylene. The target dendritic molecules, **C1-TP**, **C2-TP**, and **C-DTP**, are well soluble in common organic solvents such as, CH_2Cl_2 THF, ethylacetate, so that they were easily isolated and purified by column chromatography, and recrystallized to reach an excellent purity for OLEDs application. The chemical structures and the monodispersity of these compounds were verified using ^{1}H and ^{13}C NMR spectroscopy, and matrix-assisted laser desorption ionization time-of-flight (MALDI-TOF) mass spectrometry.

Photophysical Properties. The photophysical properties of the molecules were examined by UV−vis absorption and photoluminescence spectra in CH_2Cl_2 and toluene (Table 1). As shown in Figure 1, **TP** exhibits two major electronic absorption bands: $\pi-\pi^*$ transition at 300−350 nm and charge transfer (CT) transition at 430−530 nm.[4,6] Two extra absorption bands in the range of 280−370 nm are detected for **C1-TP**, **C2-TP**, and **C-DTP** because of the presence of carbazole units,[19] which overlap with the $\pi-\pi^*$ transition of the core. It is obvious that the absorption spectra of **C1-TP**, **C2-TP** and **C-DTP** exhibited a large red shift of 30−40 nm compared with that of the reference compound **TP**, which could be derived from the extended π conjugation in these dendritic molecules. It should be noted that the absorption intensity of the long wavelength band is much lower than that of the short wavelength absorption for all these thienopyrazine-based compounds. Upon photoexcitation, all four compounds transmit red fluorescence in dilute solutions. In toluene solution, the parent compound **TP** exhibits a broad fluorescence with the peak at 597 nm and a quantum yield of 60.5%. With introducing the carbazole groups to the surface of dendrimers, the emission peak of **C1-TP** red-shifted to 639 nm and its fluorescent quantum yield dramatically decreased to 17.3%. This should be resulted from the fact that the carbazole groups act as electron donor and quench the excited state of the

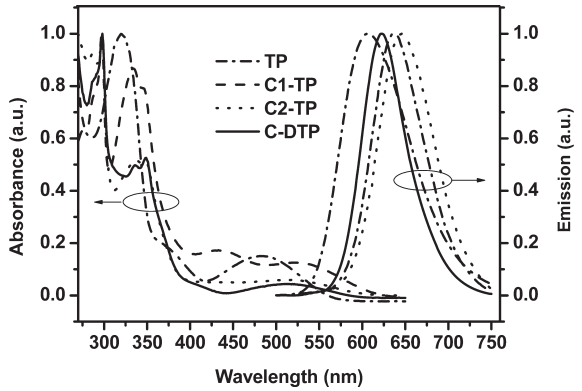

Figure 1. UV−vis absorption and photoluminescence spectra of **TP**, **C1-TP**, **C2-TP**, and **C-DTP** in CH_2Cl_2 solution (1×10^{-5} mol L^{-1}, λ_{exc} = 470 nm).

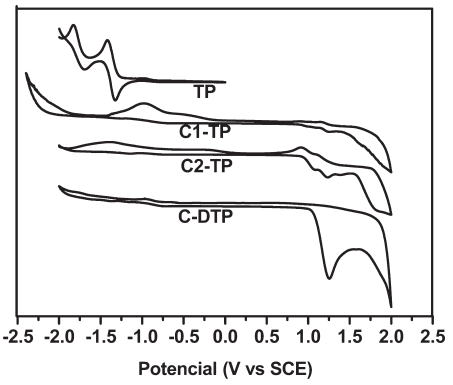

Figure 2. Cyclic voltammograms of the thieno[3,4-*b*]pyrazine derivatives (scan rate 50 mV S^{-1}, in CH_2Cl_2).

thieno-[3,4-b]-pyrazine core via photoinduced intramolecular charge transfer (ICT) to the core which serves as the electron acceptor. The generated charge transfer state possesses lower energy than that of the thieno-[3,4-b]-pyrazine fluorophore, thus **C1-TP** exhibits lower-energy fluorescence than the parent **TP**. The bathochromic effect in emission spectra and the decrease in quantum yield due to photoinduced ICT process are common phenomena for organic compounds.[26,27] With increasing the carbazole dendron generation from **C1-TP** to **C2-TP**, the emission peak shifted to shorter wavelength at 630 nm, and the fluorescent quantum yield increased to 26.7%. These observations indicate that the ICT effect in **C2-TP** is not as strong as in **C1-TP** and the fluorescence quenching in **C2-TP** becomes weaker than that in **C1-TP**. Earlier reports on carbazole dendrimers demonstrated that the substitution of the carbazole to carbazole could lead to π-polarization[32,33] type electron-withdrawing effect, i.e., when the carbazole binds to another carbazole, the outer layer of carbazole possesses a higher electron density.[16] This is probably the reason for the lower ICT efficiency of **C2-TP** compared to **C1-TP**. The ICT efficiency in donor−spacer−acceptor dyes is also dependent on the average distance between the electron donor and acceptor.[26] With further increasing the distance between the carbazole donors and the core acceptor by inserting the bulky polyphenyl group, the emission peak of **C-DTP** further hypsochromic shifted to 613 nm and its fluorescent quantum yield increased to 42.5%, which is close to that of the parent **TP**. It should be pointed out that the ICT is not the exclusive reason for the decreased quantum yield in these dendritic molecules. The increase of nonradiative decay of the excited state caused by the presence of more groups and chemical bonds in these dendritic molecules should be at least partially responsible for the decline of quantum yield. The fluorescence quenching caused by carbazole dendrons would be acceptable if their perfect site-isolation effect on the planar emissive core as well as the potential charge transporting capability are taken into account.

In addition to the spectral shift and the variation of the fluorescent quantum yield, the introduction of these carbazole dendrons also results in the spectral narrowing. As shown in Figure 1 and Table 1, the PL spectrum of the parent compound **TP** has a full width at half-maximum (fwhm) of 90 nm, while it became as narrow as 60−70 nm for the three dendritic molecules. The spectral narrowing observed in the dendritic molecules should be attributed to the fact that the intermolecular interaction between the planar emissive cores are dramatically eliminated due to the site-isolation effect of the bulky dendrons. Apparently both the red shift and the spectral narrowing caused by the introduction of carbazole dendrons are favorable to saturated red fluorescence for these dendritic molecules. For each compound, the fluorescence peak shifts to red and the quantum yield becomes lower if the solvent changes from toluene to CH_2Cl_2. This is probably ascribed to the dipolar quenching that could occur in polar solvents.[4]

As shown in Figure 1, there is a slight overlap between the absorption and emission spectra of these thieno-[3,4-*b*]-pyrazine derivatives. Calculated from the positions of the absorption maximum (weak band at longer wavelength) and the fluorescence maximum, the Stokes Shifts are as large as 122, 125, 125, and 107 nm for **TP**, **C1-TP**, **C2-TP**, and **C-DTP**, respectively. Such large Stokes shifts are especially valuable for light-emitting materials used in nondoped OLEDs because each emissive molecule is densely surrounded in the neat film and the absence of self-absorption will definitely facilitate efficient light output from the device.

Electrochemical Properties. The redox behavior of these thieno-[3,4-*b*]pyrazine derivatives was investigated by means of cyclic voltammetry measurements. As shown by the cyclic voltammograms in Figure 2, the reference compound **TP** exhibits two reversible reduction waves, which should be assigned to two step one-electron reductions of the thieno-[3,4-*b*]-pyrazine core. No oxidation was observed for it. The detection of only reduction processes indicates the electron-deficient and n-type feature of the thieno-[3,4-*b*]-pyrazine chromophore, despite that most thiophene-containing species usually reveal electron-donating and p-type nature.[4,34,35] This is consistent with the above observation that the thieno-[3,4-*b*]-pyrazine core serves as electron acceptor in the dendritic molecules. With introduction of the carbazole dendrons, multiple oxidation waves were detected for **C1-TP**, **C2-TP** and **C-DTP**. It would be reasonable to assign the reduction to the thieno-[3,4-*b*]-pyrazine core and the oxidation to the peripheral carbazole groups or even to the polyphenyl moieties. The oxidation waves for **C1-TP**, **C2-TP** and **C-DTP** are comparable to each other. The oxidation current of **C2-TP** is stronger than that of **C1-TP** because **C2-TP** has more electron donating groups. The highest occupied molecular orbital (HOMO) energy levels were calculated from the onset potential of the first oxidation wave for **C1-TP**, **C2-TP** and **C-DTP**. The optical bandgaps for these compounds were determined by absorption edge technique.[36] Accordingly, their

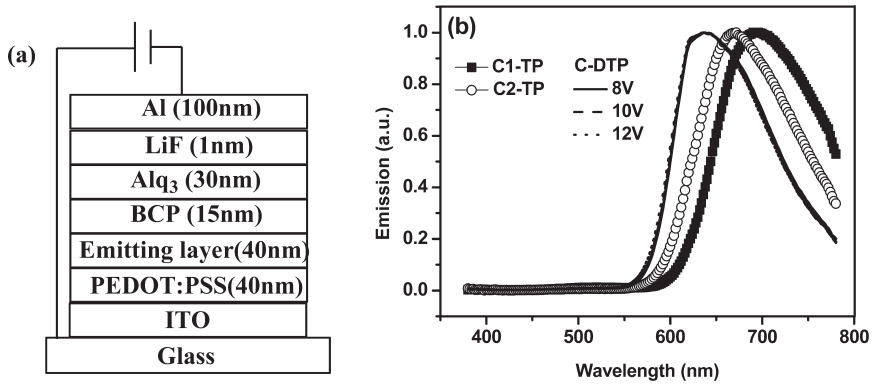

Figure 3. (a) Schematic diagram of the EL device configuration and (b) the EL spectra of the **C1-TP**, **C2-TP**, and **C-DTP**-based OLEDs.

lowest unoccupied molecular orbital (LUMO) energy levels are calculated by subtracting the gaps from the HOMO energies. For the parent compound **TP**, the LUMO level was calculated from the first reduction reaction, and the HOMO level is obtained as the sum of the LUMO energy and the optical gap. The detailed electrochemical and electronic data for these compounds are listed in Table 1.

Electroluminecent Properties. In order to evaluate the electroluminescent properties, all these thieno-[3,4-*b*]-pyrazine derivatives were used as the neat emitting layer (EML) to fabricate nondoped OLEDs. The OLEDs have a configuration of ITO/PEDOT:PSS (40 nm)/EML (40 nm)/BCP (15 nm)/Alq_3 (30 nm)/LiF (1 nm)/Al (100 nm) (Figure 3a) where PEDOT:PSS (poly(3,4-ethylenedioxythiophene):poly(styrene sulfonate)) acts as the hole injecting and transporting layer, BCP (2,9-dimethyl-4,7-diphenyl-1,10-phenanthroline) as the hole and exciton blocking layer, Alq_3 (tris(8-hydroxyquino) aluminum) as the electron transporting layer, and ITO (indium tin oxide) and LiF/Al as anode and cathode respectively. On the basis of the excellent solubility of **C2-TP** and **C-DTP** in common organic solvents, high-quality neat films without pinholes can be obtained by spin coating their solutions in chlorobenzene to form the EML. As an exception, the **TP** and **C1-TP** films are deposited by vacuum evaporation since a film of significant thickness could not be obtained via solution process because of the low molecular weight and limited solution viscosity.

The thickness of each functional layer was carefully tuned in order to confine the charge recombination zone into the EML and to achieve the pure emission from these thieno-[3,4-*b*]-pyrazine molecules without spectral contamination from adjacent layers. The film thickness in above configuration is chosen after optimization. As shown in Figure 3b, all these OLEDs based on dendritic materials emit saturated red EL with peaks at 690, 670, and 636 nm and CIE coordinates of (0.67, 0.31), (0.65, 0.33), and (0.66, 0.34) for **C1-TP**, **C2-TP**, and **C-DTP**, respectively. The EL spectra and CIE coordinates almost keep unchanged with increasing driving voltage, which offers better device operation compared to red OLEDs with dopants in which the color changes with voltage.[37] Compared with their PL spectra in CH_2Cl_2 solutions, a large red shift of 44 and 36 nm was observed in EL spectra for **C1-TP** and **C2-TP**, respectively. Although the spectral red shift is frequently observed in EL of many light-emitting materials due to electrical field effect on the excited states, such a large red shift for **C1-TP** and **C2-TP** implies

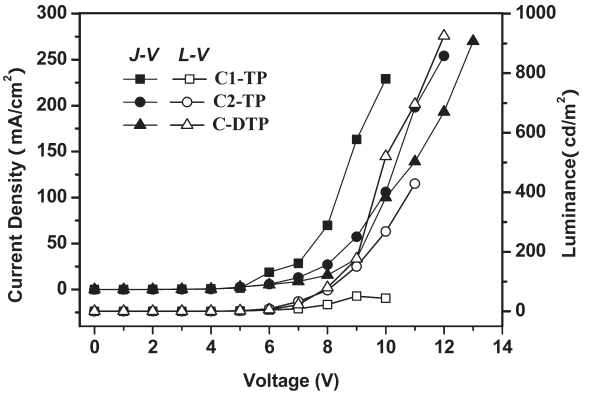

Figure 4. Luminance−voltage−current density ($L-V-J$) characteristics for **C1-TP**, **C2-TP**, and **C-DTP**-based OLEDs.

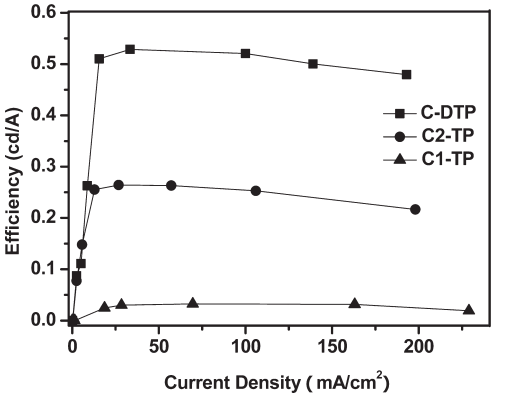

Figure 5. Plots of luminance efficiency versus current density for **C1-TP**, **C2-TP**, and **C-DTP**-based OLEDs.

that the site-isolation effect of the carbazole dendrons on the emissive core is not sufficient enough to completely eliminate the intermolecular interaction, which is known to be an important reason for the spectra shift. Although a smaller red shift of 13 nm was observed for **C-DTP**, further confirming that the larger dendrons in **C-DTP** molecules provide significant site-isolation effect on the core so that unwanted intermolecular interactions can be inhibited. For **C2-TP** and **C-DTP**-based OLEDs, their CIE coordinates are very close to the coordinates (0.64, 0.33) of

Table 2. Electroluminescent Data of OLEDs Based on Compounds C1-TP, C2-TP, and C-DTP

compd	V_{on} (V)	L_{max} (cd/m^2) (at the voltage (V))	η_{max} (cd/A) (at mA/cm^2)	η (cd/A) (at 100 mA/cm^2)	λ_{max} (nm)	$\Delta\lambda$ (nm) [a]	CIE (x, y)
C1-TP	5	51 (10)	0.032 (69.6)	0.032	690	44	0.67, 0.31
C2-TP	5	428 (11)	0.264 (26.8)	0.25	672	36	0.66, 0.33
D-TTP	4.5	925 (11.5)	0.529 (33.4)	0.52	636	13	0.66, 0.34

[a] The red shift of EL peak relative to PL in CH_2Cl_2.

the standard red color of the National Television System Committee (NTSC).[38]

The luminance−voltage-current density ($L-V-J$) characteristics and the efficiency curves for dendrimers **C1-TP**, **C2-TP**, and **C-DTP**-based OLEDs are displayed in Figure 4 and Figure 5, respectively. And the detailed EL data are summarized in Table 2. Both **C1-TP** and **C2-TP** based OLEDs turned on (to deliver a brightness of 1 cd m^{-2}) at a voltage of 5 V, whereas the **C-DTP** device turned on at a lower voltage of 4.5 V. At a given voltage, the **C1-TP** based OLED produced the highest current density but the lowest brightness and lowest efficiency among these three OLEDs. This implies that the severe ICT once again takes effect to quench the excited states of the emissive core which are generated through charge recombination in OLED. With increasing carbazole dendron generation, the device performance for **C2-TP** is improved with higher brightness and emission efficiency than **C1-TP**. With further increasing the dendron dimension, **C-DTP**-based OLED offered a further improved performance. It is apparent that the EL brightness at a given voltage for **C-DTP** device is much higher than those of **C1-TP** and **C2-TP** devices over the whole detected voltage range, suggesting that the incorporation of polyphenyl groups between the red core and carbazole groups significantly contributed to lower the ICT efficiency and consequently increase the luminance of the OLEDs. The **C-DTP** device reaches a maximum brightness of 925 cd m^{-2} (at 11.5 V), much higher than 51 cd m^{-2} (at 10 V) and 428 cd m^{-2} (at 11 V) for **C1-TP** and **C2-TP** devices, respectively. As illustrated in Figure 5, the luminance efficiency of **C-DTP** device reaches a maximum of 0.53 cd A^{-1} at 33 mA cm^{-2}, and almost keeps constant at a higher current density of 200 mA cm^{-1}.

As mentioned above, the vacuum-deposited thieno-[3,4-*b*]-pyrazine derivative in previous report[4] could reach a maximum luminance efficiency of 0.34 cd A^{-1} and brightness of 1766 cd m^{-2} with CIE (0.65, 0.33). A higher efficiency of 0.65 cd A^{-1} was possible but at the expense of the emission color shifting to orange (0.59, 0.33). Evidently the present thieno-[3,4-*b*]-pyrazine derivative **C-DTP** has higher emission efficiency than the vacuum-deposited counterparts on the premise of saturated red emission, despite the lower brightness. In addition, these dendritic thieno-[3,4-*b*]-pyrazine derivatives are superior in terms of device fabrication because solution processing is a much easier method. As far as we know, the performance of the present dendritic molecule **C-DTP** is also comparable with those solution-processable red fluorescent dendrimers reported in recent years.[3,7,39,40]

In contrast to the good performance of these dendritic materials, the OLEDs containing the parent compound **TP** as the emitting layer always produced a mixed emission from both **TP** and Alq_3 with poor intensity, although great efforts have been taken to tune the thickness of each functional layer. This may result from the unbalanced charge transporting state within the device and the strong unwanted intermolecular interaction of more planar **TP** molecules in solid state. Once again it is implied that the charge transporting bulky dendrons indeed play an essential role to improve emission performance in **C1-TP**, **C2-TP**, and **C-DTP**.

CONCLUSIONS

We demonstrated the design strategy and synthesis of a group of novel thieno-[3,4-*b*]-pyrazine cored dendrimers for OLEDs application. The attachment of oligo-carbazole dendrons to the thieno-[3,4-*b*]-pyrazine emissive core enabled this small molecule fluorophore to be solution processable to form good-quality thin films and to be charge transportation active. Meanwhile, the fluorescence quenching caused by ICT in these donor−spacer−acceptor systems becomes less significant with increasing dendron generation and introducing polyphenyl spacer. As a result, the solution-processed OLEDs using these dendritic thieno-[3,4-*b*]-pyrazine derivatives as nondoped emitting layer exhibited pure and saturated red fluorescence and provided comparable performance with those of small molecular analogues via vacuum deposition. Extraordinarily large Stokes Shift, sufficient site-isolation effect of dendrons on the planar emissive core, and proper charge transporting ability combine to be for the root causes for the improved performance of these dendritic thieno-[3,4-*b*]-pyrazine derivatives. This report provides a practical strategy to decorate the highly efficient but planar luminophors to be suitable for application in solution-processable and nondoped OLEDs.

ASSOCIATED CONTENT

Supporting Information. Additional figures (PDF). This material is available free of charge via the Internet at http://pubs.acs.org.

AUTHOR INFORMATION

Corresponding Author

*Fax: +86 411 84986233. E-mail: jiuyanli@dlut.edu.cn .

ACKNOWLEDGMENT

We thank the National Natural Science Foundation of China (U0634003, 20704002, 20923006, and 21072026), the Ministry of Education for the New Century Excellent Talents in University (Grant NCET-08-0074), the NKBRSF (2009CB220009), and the Fundamental Research Funds for the Central Universities (DUT10LK16) for financial support of this work.

REFERENCES

(1) Bordeau, G.; Lartia, R.; Teulade-Fichou, M.-P. *Tetrahedron Lett.* **2010**, *51*, 4429.

(2) Wu, W. C.; Yeh, H. C.; Chan, L. H.; Chen, C. T. *Adv. Mater.* **2002**, *14*, 1072.

(3) Wang, J. L.; Zhou, Y.; Li, Y. F.; Pei, J. *J. Org. Chem.* **2009**, *74*, 7449.
(4) J-Thomas, K. R.; Lin, J. T.; Tao, Y. T.; Chuen, C.-H. *Adv. Mater.* **2002**, *14*, 822.
(5) Burroughes, J. H.; Bradley, D. D. C.; Brown, A. R.; Mackay, R. N.; Marks., K.; Friend, R. H.; Burns, P. L.; Holmes, A. B. *Nature* **1990**, *347*, 539.
(6) Yang, Y.; Zhou, Y.; He, Q. G.; He, C.; Yang, C. H.; Bai, F. L.; Li, Y. F. *J. Phys. Chem. B.* **2009**, *113*, 7745.
(7) Burn, P. L.; Lo, S.-C.; Samuel, I. D. W. *Adv. Mater.* **2007**, *19*, 1675.
(8) Li, J Y; Liu, D. *J. Mater. Chem.* **2009**, *19*, 7584–7591.
(9) Hwang, S.-K.; Moorefield, C. N.; Newkome, G. R. *Chem. Soc. Rev.* **2008**, *37*, 2543.
(10) Li, J. Y.; Liu, D.; Ma, C.; Lengyel, O.; Lee, C.-S.; Tung, C.-H.; Lee, S.-T. *Adv. Mater.* **2004**, *16*, 1538.
(11) Wong, W. Y.; Ho, C. L.; Gao, Z. Q.; Mi, B. X.; Chen, C. H.; Cheah, K. W.; Lin, Z. *Angew. Chem., Int. Ed.* **2006**, *45*, 7800.
(12) Li, J. Y.; Ma, C.; Tang, J.; Lee, C.-S.; Lee, S. T. *Chem. Mater.* **2005**, *17*, 615.
(13) Akira, B.; Ken, O.; Wolfgang, K.; Rigoberto, C. A. *J. Phys. Chem. B* **2004**, *108*, 18949.
(14) Velasco, D.; Castellanos, S.; López, M.; Calahorra, F. L.; Brillas, E.; Julia, L. *J. Org. Chem.* **2007**, *72*, 7523.
(15) Xu, T. H.; Lu, R.; Qiu, X. P.; Liu, X. L.; Xue, P. C.; Tan, C. H.; Bao, C. Y.; Zhao, Y. Y. *J. Org. Chem.* **2006**, 4014.
(16) Albrecht, K.; Yamamoto, K. *J. Am. Chem. Soc.* **2009**, *131*, 2244.
(17) Ding, J. Q.; Lu, J. H.; Cheng, Y. X.; Xie, Z. Y.; Wang, L. X.; Jing, X. B.; Wang, F. S. *Adv. Funct. Mater.* **2008**, *18*, 2754.
(18) Ding, J. Q; Lu, J. H.; Cheng, Y. X.; Xie, Z. Y.; Wang, L. X.; Jing, X. B.; Zhang, H. Q.; Wang, S. M.; Li, Y. Q.; Zhang, B.; Du, C. X.; Wan, X. J.; Chen, Y. S. *Tetrahedron* **2009**, *65*, 4455.
(19) Jiang, J.; Jiang, C.; Yang, W.; Zhen, H.; Hung, F.; Cao, Y. *Macromolecules* **2005**, *38*, 4072.
(20) J-Thomas, R. J. K; Lin, T.; Tsai, C.-M.; Lin, H.-C. *Tetrahedron* **2006**, *62*, 3517.
(21) Casalbore-Miceli, G.; Esposti, A. D.; Fattori, V.; Marconi, G.; Sabatini, C. *Phys. Chem. Chem. Phys.* **2004**, *6*, 3092.
(22) Kondakov, D. T. *J. Appl. Phys.* **2008**, *104*, 84520.
(23) Chuen, C. H.; Tao, Y. T. *Appl. Phys. Lett.* **2002**, *81*, 4499.
(24) Lee, Y. T.; Chiang, C. L.; Chen, C. T. *Chem. Commun.* **2008**, 217.
(25) Moorthy, J. N.; Venkatarishnan, P.; Huang, D.-F.; Chow, T. J. *Chem. Commun.* **2008**, 2146.
(26) Qu, J. Q.; Pschirer, N. G.; Liu, D. J.; Stefan, A.; Schryver, F. C. D.; Mullen, K. *Chem.—Eur. J.* **2004**, *10*, 528.
(27) Ohkita, H.; Benten, H.; Anada, A.; Noguchi, H.; Kido, N.; Ito, S.; Yamamoto, M. *Phys. Chem. Chem. Phys.* **2004**, *6*, 3977.
(28) Neugebauer, F. A.; Fisher, H.; Bamberger, S.; Smith, H. O. *Chem. Ber.* **1972**, *105*, 2686.
(29) Bauer, R.; Liu, D.; Heyen, A. V.; Schryver, F. D.; Feyter, S. D.; Muellen, K. *Macromolecules* **2007**, *40*, 4753.
(30) Liu, D.; Ren, H. C.; Li, J. Y.; Tao, Q.; Gao, Z. X. *Chem. Phys. Lett.* **2009**, *482*, 72–76.
(31) Kastler, M.; Schmidt, J.; Pisula, W.; Sebastiani, D.; Mullen, K. *J. Am. Chem. Soc.* **2006**, *128*, 9526.
(32) Neuvonen, K.; Fulop, F.; Neuvonen, H.; Koch, A.; Kleinpeter, E.; Pihlaja, K. *J. Org. Chem.* **2003**, *68*, 2151.
(33) Fadhil, G. F.; Radhy, H. A.; Perjessy, A.; Samalikova, M.; Kolehmainen, E.; Fabian, W. M. F.; Laihia, K.; Sustekova, Z. *Molecules* **2002**, *7*, 833.
(34) Roncali, J. *Chem. Rev.* **1997**, *97*, 173.
(35) Shahid, M.; Ashraf, R. S.; Klemm, E.; Sensfuss, S. *Macromolecules* **2006**, *39*, 7844.
(36) Zhou, Y.; He, Q. G.; Yang, Y.; Zhong, H. Z.; He, C.; Sang, G. Y.; Liu, W.; Yang, C. H.; Bai, F. L.; Li, Y. F. *Adv. Funct. Mater.* **2008**, *18*, 3299.
(37) Kwong, R. C.; Sibley, S.; Dubovoy, T.; Baldo, M.; Forrest, S. R.; Thompson, M. E. *Chem. Mater.* **1999**, *11*, 3709.
(38) Chen, S. Y.; Xu, X. J.; Liu, Y. Q.; Yu, G.; Sun, X. B.; Qiu, W. F.; Ma, Y. Q.; Zhu, D. B. *Adv. Funct. Mater.* **2005**, *15*, 1541.
(39) Pan, J. F.; Zhu, W. H.; Li, S. F.; Zeng, W. J.; Cao, Y.; Tian, H. *Polymer* **2005**, *46*, 7658.
(40) Kim, G. W.; Cho, M. J.; Yu, Y. J.; Kim, Z. H; Jin, J.; Kim, D. Y.; Choi, D. H. *Chem. Mater.* **2007**, *19*, 42.